

# Effect of the Blast Load on FRP Panels and Analysis of Resistance

Hossein Rezaei, Fereydoon Omidinasab\*, Peyman Beiranvand and Mohammad Hossein Naserifard

Department of Civil Engineering, Lorestan University, Khorram abad, Iran;  
Rezaei.hossewin34@gmail.com, Omidinasabfereydon1@gmail.com, Peymanbeiranvand12@gmail.com

## Abstract

A concise state-of-the-art survey of fiber-reinforced polymer composites for construction applications in civil engineering is presented. The paper is organized into separate sections on structural shapes, bridge decks, internal reinforcements, externally bonded reinforcements, and standards and codes. One of these uses is the blast reduce. This is attributed to FRP ability of absorbing considerable amount of energy relative to their low density. In this research work, the finite element package ANSYS is used to study the behavior of hexagonal and squared steel sandwich panels under the explosive effects of different amounts of trinitrotoluene (TNT). The results of finite element modeling of a specific configuration are initially validated by comparing them with the experimental results from literature. Afterwards, several configurations including different geometrical properties of the wall are investigated and the results are compared with the original model. Finally, the effectiveness of the core shape and wall thickness and Length, Width and Height are discussed, and conclusions are made.

**Keywords:** Blast Load, Fiber Reinforced Polymers, Finite Element Modeling, Sandwich Panels

## 1. Introduction

In the last 200 years, rapid advances in construction materials technology have enabled civil engineers to achieve impressive gains in the safety, economy, and functionality of structures built to serve the common needs of society. Through such gains, the health and standard of living of individuals are improved. To mark the occasion of the 150th anniversary of the American Society of Civil Engineers (ASCE), this paper reviews a class of structural materials that has been in use since the 1940s but only recently has won the attention of engineers involved in the construction of civil structures—fiber-reinforced polymer (or fiber reinforced plastic) (FRP) composites. The earliest FRP materials used glass fibers embedded in polymeric resins that were made available by the burgeoning petrochemical industry following World War II. The combination of high-strength, high-stiffness structural fibers with low-cost, lightweight, environmentally resistant polymers resulted

in composite materials with mechanical properties and durability better than either of the constituents alone. Fiber materials with higher strength, higher stiffness, and lower density, such as boron, carbon, and aramid, were commercialized to meet the higher performance challenges of space exploration and air travel in the 1960s and 1970s. At first, composites made with these higher performing fibers were too expensive to make much impact beyond niche applications in the aerospace and defense industries. Work had already begun in the 1970s, however, to lower the cost of highperformance FRPs and promote substantial marketing opportunities in sporting goods. By the late 1980s and early 1990s, as the defense market waned, increased importance was placed by fiber and FRP manufacturers on cost reduction for the continued growth of the FRP industry. As the cost of FRP materials continues to decrease and the need for aggressive infrastructure renewal becomes increasingly evident in the developed world, pressure has mounted for the use of these new materials to meet higher

\*Author for correspondence

public expectations in terms of infrastructure functionality. Aided by the growth in research and demonstration projects funded by industries and governments around the world during the late 1980s and throughout the 1990s, FRP materials are now finding wider acceptance in the characteristically conservative infrastructure construction industry. Hence, a brief review of the development, state of the art, and future of these promising construction materials is a timely and appropriate marker for the 150th anniversary of the ASCE.

Nowadays concrete-filled steel structures have been extensively used all around the world because of being more economic, less deformation in lateral loading and reducing the dimensions of the section with the same load capacity, less weight and as result having all suitable characteristics of concrete and steel. These types of sections have also ductility, larger energy absorption capacity and power and ultimately fire resistance. Explosion is the result of sudden release of energy that can be as combusting gases, nuclear explosion or as result of different types of bomb. TNT is usually used as a reference for determining explosion power. Of main characteristics of explosion that leads to pushing force on structure, randomness of explosive situation, forces' dynamicity and transience of forces and low impact (between a few milliseconds to several seconds) can be mentioned. When there is an explosion, energy is suddenly released. The effect of releasing this energy can be divided into two parts of thermal radiations and wave propagation in land and air that in current paper, only the first section is investigated. Steel is a material with high thermal lead however when it is affected by fire, its resistance will be rapidly decreased. Blast responses are usually more noticeable for vital structures and protection ones. By loading concrete-filled steel columns, restricted concrete prevents local buckling to the inside steel wall because there will be restriction mood in concrete and therefore it will be pressured triaxially and member's rupture will be deformed from brittle state to plastics compared to concrete columns.

## 2. Numerical Model Validation

A numerical model has been simulated based on the experimental work conducted by Hoemann at Tyndall Air Force Base, Florida<sup>2</sup>, where the obtained results were compared to validate the numerical model. The numerical model has been simulated using dynamic nonlinear

explicit software ANSYS AUTODYN<sup>18-20</sup>. The software is used in solving fluid dynamics equations and can be used to simulate three-dimensional blast wave propagation with multiple reflections and refraction. Figure 1 shows a schematic of the numerical model, including all blast wave characteristics that are usually associated with the explosion. Similar to the experimental investigation, the center of explosion is located at 10.7 m from the simulated panel and elevated at 1.8 m from the ground surface.

Figure 2 shows the pressure-time history of the experimental field test and the numerical model. In the experimental tests, four gauges were installed in the field (R1 to R4), where gauge R3 was considered as a defective gauge. In the numerical model, the peak pressure value is 1215 kPa which is close to the average pressure value of the 3 field pressure gauges. Figures 3(a) to 2(d) show the experimental and numerical deflection time histories of the four panels (W1 to W4) considered. It is worth mentioning that W1 and W2 have the same dimensions and different inner core configurations. Whereas, W3 and W4 have the same inner core configurations as W1 and W2 but are different in dimensions. Throughout the experiment, W1, W2, W3 and W4 were filled with sand. The Figure 3 show that the numerical model agrees well with the experimental test, expect for panel W3 where a discrepancy has been noticed after reaching the peak

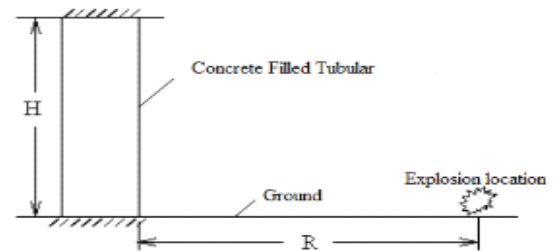


Figure 1. Schematic of the numerical model.

displacement value. This can be due to the failure of the clamping anchorage joints that took place at the experimental test after the panels started the rebound phase. Such failure has not been taken in consideration during the numerical simulation. As the boundary conditions remain the same during the analysis.

### 3. Proposed FRP Sandwich Panel

The proposed FRP panel is formed of a new inner core configuration. This configuration is formulated from a combination of woven and honeycomb shapes. In order to compare the analyzed results, the modeled FRP panel has the same dimension and has been filled with sand as W3 and W4. Also, the modeled FRP panel has maintained the same amount of FRP material as used in

W3 and W4. This panel is 1800 mm height (Y-axis), 2600 mm width (Z-axis) and 360 mm (X-axis) thickness. The inner core configuration is formed from sinusoidal core layers similar to the experimental panels (W1 to W4), which are used as layers or cutting strips. Figure 4 depicts the FRP sandwich panel with the two main inner core configurations considered in the analyses. Configuration (1) consists of strips that are perpendicularly interlaced, forming the woven shape. This configuration is represented by “WV2-1 strips”, which consist of two strips from the sinusoidal layer in the longitudinal direction and one fill from the sinusoidal strip in the transverse direction. On the other hand, configuration (2) represented by “RW axis” - is formed of sinusoidal layers that are separated by flat layers in between, forming a honeycomb shape. The inner core configurations are formed of four layers of WV2-1 and one layer of RW with a flat layer separating each two layers. These four layers are divided into two Layers at the Top (TL) with a total thickness of 110 mm and other two Layers at the Bottom (BL) with the same total thickness, while the RW layer is placed in between the top and bottom layers with thickness of 120 mm.

The proposed FRP panel aims to enhance the behavior of the FRP panel when subjected to blast loading. This enhancement can be achieved by decreasing the panel’s peak deflection and increasing its energy dissipation. The importance of the panel’s peak deflection is that it can represent the panel’s level of damage<sup>21,22</sup>. For the simulated test panels, W3 has a peak deflection value of 72 mm and energy absorption of 121 J. While, W4 has a peak deflection value of 163 mm and energy absorption of 268 J. Figure 5 shows the time history of the central point deflection of the FRP panels of the proposed panel (W5) with the simulated test panels W3 and W4. In the figure, it can be seen that the peak deflection of the new proposed panel W5 is 67 mm reduced by 7% comparing to W3, in addition to realizing an increased the arrival time of peak deflection. While, under the same conditions, W5 energy dissipation is 256 J. This represents a 111% increase compared to W3 and 4% decrease compared to W4. Therefore, W5 gets the advantage of having low peak deflection as W3 and the high energy absorption as W4.

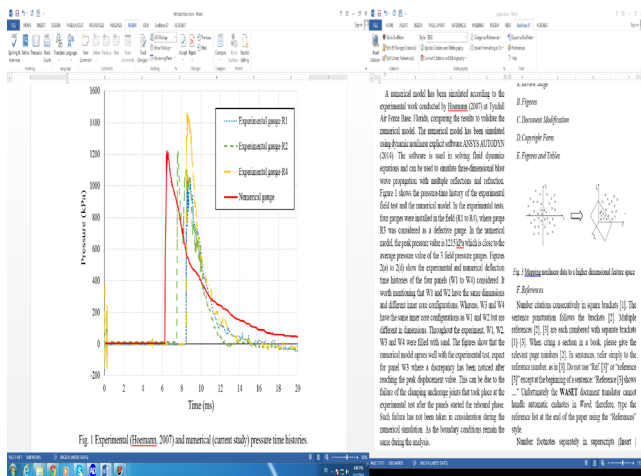


Figure 2. Experimental<sup>2</sup> vs. numerical pressure time histories.

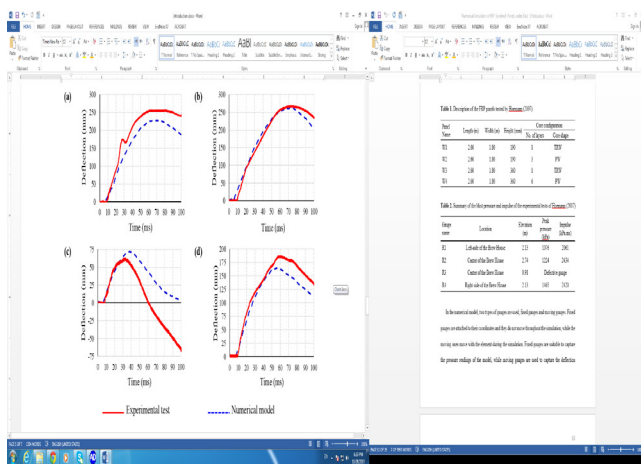


Figure 3. Validation of numerical model against experimental results<sup>2</sup> for (a) W1, (b) W2, (c) W3 and (d) W4.

### 4. Parametric Study

In this section, a parametric analyses have been carried out on the WV2-1 layers to better understand the

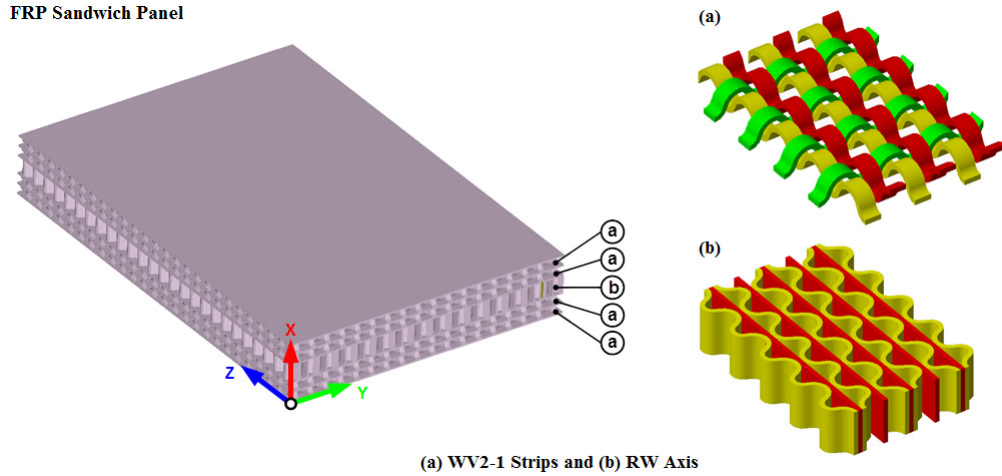


Figure 4. Inter core configurations of the FRP sandwich panels..

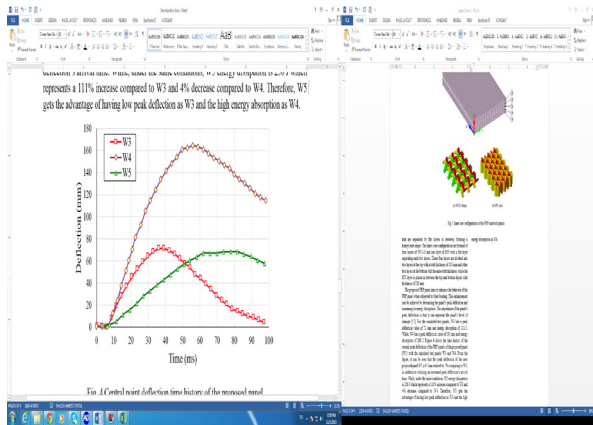


Figure 5. Central point deflection time history of the proposed panel.

performance of the proposed FRP panel against blast loads. The energy dissipated by the panel, the maximum deflection of the panel and the  $E/\Delta$  ratio have been studied.  $E/\Delta$  ratio is defined as the total energy dissipated by the panel relative to the panel's maximum deflection at the center point. The higher value of  $E/\Delta$  ratio indicates that the panel would be able to absorb a higher amount of energy with less deformations and less amount of damage. Figure 6 shows schematics of the elevation and cross section of the WV2-1 strips, where  $t$  is the thickness of the sinusoidal and flat layers,  $h$  is the height of sinusoidal layer,  $L$  represents a single sinusoidal wave length and  $W$  is the width of one strip. It is worth mentioning that W5 has the same sinusoidal and flat layers' dimensions and amount of material - as the experimental panels.

Therefore, all the results obtained from the other analyzed panels and the amount of used material

#### 4.1 Effect of Length, Width and Height

Table 1 illustrates the effect of changing the layers' height ( $H$ ), wave length ( $L$ ) and the strip width ( $W$ ) on the panel's performance. Nine panels have been studied including W5. The three different heights ( $H$ ) considered in this study are 50, 30 and 110 mm. In order to maintain the total thickness of the TL and BL constant equals to

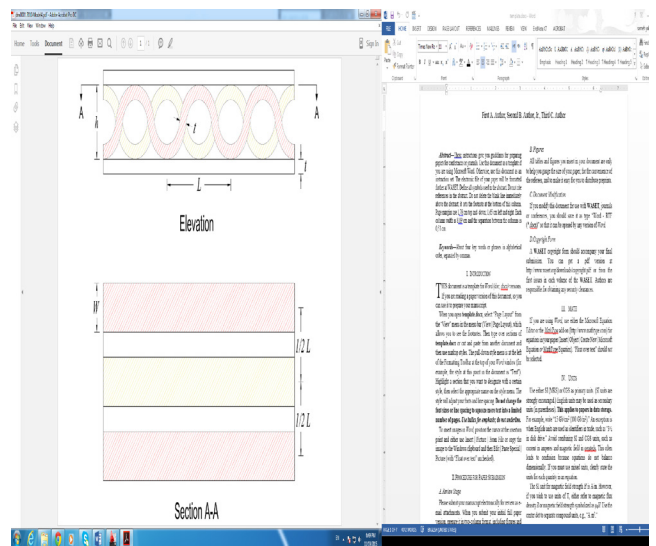


Figure 6. Schematic of a woven core sandwich panel.

110 mm, the change in height is always associated with a change in the number of layers. In the table, the “No. of layers” column represents the total number of layers in both TL and BL. The increase/decrease in the material weight (% Mass) - as a result of the dimensions’ change - is illustrated in the table. From the Table 1, it can be seen that decreasing the height leads to better performance, as the energy dissipation increases by up to 25% and panels’ peak deflection decreases by up to 13.4%. Moreover, decreasing the wave length slightly enhances the performance of the panels. Comparing W6 with W5, W9 with W8 and W12 with W11, the energy dissipation increases by 2.7%, 2.9% and 6.9%, respectively. While the panels’

peak deflection decreases by 1.5%, 3.3% and 7.3%, respectively. As long as the nine analyzed panels have different weights of material, thus the comparison between these panels is merely considered as guidelines.

## 4.2 Effect of Thickness

Table 2 illustrates the effect of changing layers’ thickness (T) on the panel’s performance. W5 and W8 panels are analyzed under four different thickness values: 10, 9, 8 and 7 mm. Analyzed results show that decreasing the thickness of the modeled panels does not affect the energy dissipation, where a maximum of 0.8% variation

**Table 1.** Effect of length, width and height variations

Panel	h (mm)	L (mm)	W (mm)	t (mm)	No. of layers	% Mass	Energy dissipation(J)	$\Delta_{max}$ (mm)	E/ $\Delta$	% E/ $\Delta$
W5	50	100	33	10	4	-	256	67	3.8	-
W6		80	24			+6.4	263	66	4	+4.9
W7		120	40			-6.6	249	69	3.6	-5.0
W8	30	100	33		6	+42.8	311	60	5.2	+36.4
W9		80	24			+44.2	320	58	5.5	+45.2
W10		120	40			+39.7	299	62	4.8	+26.9
W11	110	100	33		2	-37.3	203	96	2.1	-44.3
W12		80	24			-27.0	217	89	2.4	-35.8
W13		120	40			-47.5	184	103	1.85	-53.0

is obtained upon changing each of the panel’s thickness. On the other hand, the panels’ peak deflection is significantly affected, where a difference of up to 19.4% is obtained. Moreover, when comparing the material weight used in the modeled panels (% Mass) with the change in energy-to-deflection ratio (% E/ $\Delta$ ), the analyses show an interesting behavior of the panels. For instance, when the material weight of W5 is decreased by 27.8%, the energy-to-deflection ratio is passively decreased to 16.1% only. As for W8, when the material weight is decreased by 28.2%, the energy-to-deflection ratio is reduced to 13.6%. Additionally, upon comparing the structural behavior of W5 and W8 (with t = 7 mm), the energy-to-deflection ratio of the latter panel is increased by 17.5%; although both panels almost have the same material weight.

Therefore, it is obvious that decreasing the thickness enhances the panels’ performance. This can be attributed to the bond failure between the FRP layers that has taken place in the analyzed panels. Accordingly, decreasing the thickness of used panels does not affect the structural behavior as much as the number of bonds contacts and number of layers do.

## 5. Constant Weight

Table 3 illustrates the effect of changing the dimensions of sinusoidal and flat layers on the panel’s performance while keeping the weight of material constant. Six panels have been studied including W5. As shown in the Table

**Table 2.** Effect of thickness variations

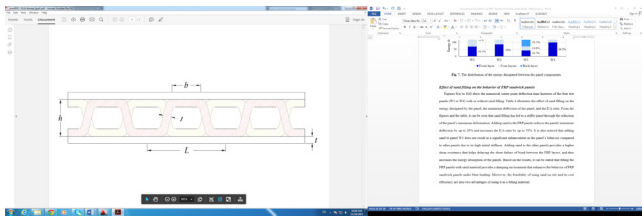
Panel	$h$ (mm)	$L$ (mm)	$W$ (mm)	$t$ (mm)	No. of layers	% Mass	Energy dissipation (J)	$\Delta_{\max}$ (mm)	E/ $\Delta$	% E/ $\Delta$
W5	50	100	33	10	4	-	256	67	3.8	-
				9		-8.8	257	72	3.6	-6.1
				8		-18.2	254	76	3.3	-12.0
				7		-27.8	255	80	3.2	-16.1
W8	30	100	33	10	6	42.8	311	60	5.2	36.4
				9		29.8	309	64	4.8	27.1
				8		16.3	310	66	4.7	23.6
				7		2.5	309	69	4.5	17.5

3, three different heights (H) have been used for each two panels. The heights used are 50, 30 and 110 mm, respectively. As for the wave lengths (L), 100 and 80 mm are used across the three different wave heights mentioned. This means that each two waves of the same height are once tested using a 100 mm wave length and once using an 80 mm wave length. The strip width (W) and layers' thickness (T) are changeable in order to maintain the same material weight. The panels of 30 mm height (W15 and W16) have resulted in a superior performance compared to panel W5. Increasing the number of layers while decreasing the layers' thickness (T) in W15 has increased the energy dissipation by 20.3% and the panels' peak deflection by 2.9%. Relatively, the energy-to-deflection ratio increases by 17.5%. While in W16, the number of the bonds contacts increases due to the decrease in wave length (L). Whereas, the number of layers increases due to the decrease in the layers' heights. Accordingly, the mentioned parameters increase the energy dissipation by 24.2% and decrease the panels' peak deflection by 1.5%. Relatively, the energy-to-deflection ratio increases by 26.8%.

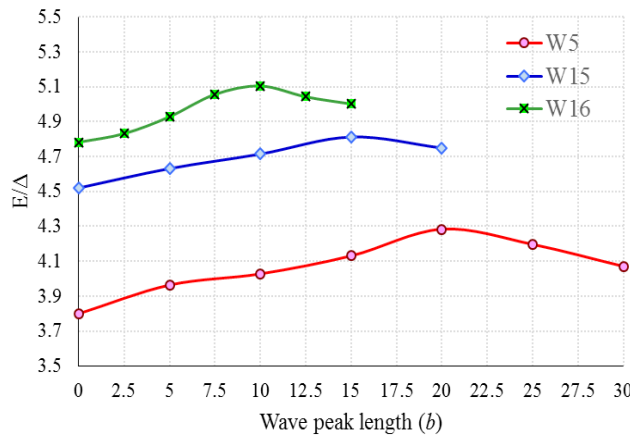
### 5.1 Effect of Wave Peak Length

Figure 7 shows schematics of the WV2-1 strips with wave peak length  $\geq 0$ . Wave peak length represented by (b) is changed to investigate its effect on the panel's performance. W5, W15 and W16 panels with the same material weight are analyzed under different wave peak length values. For W5, seven panels are studied through increasing wave peak length by 5 mm increments ranging in length from 0 to 30 mm. While for W15, five panels are studied through increasing wave peak length by 5 mm increments ranging in length from 0 to 20 mm. Finally, for W16, seven panels are studied through increasing wave peak length by 2.5 mm increments ranging in length from 0 to 15 mm. As the maximum value of wave peak length that can be reached is controlled by keeping strip layers contactless - strips are jointed only with flat layers, it is understood that the maximum peak wave length varies for each of the three studied panels W5, W15 and W16 at 30, 20 and 15 mm, respectively.

Figure 8 shows the effect of changing wave peak length on the energy-to-deflection ratio for W5, W15 and W16 panels. The results show that as the wave peak length increases, the energy-to-deflection ratio increases until it reaches the peak value then decreases gradually. Reaching



**Figure 7.** Schematic of a woven core sandwich panel with wave peak length  $\geq 0$ .



**Figure 8.** Effect of peak length variations.

the peak wave length differs from one panel to another for the three studied panels. For W5, the maximum energy-to-deflection ratio is at wave peak length of 20 mm. In comparing the increase in  $E/\Delta$  of changing the wave peak length from 0 to 20 mm, the  $E/\Delta$  increases by 12.7%. As for W15, the maximum energy-to-deflection ratio is at wave peak length of 15 mm. In comparing the increase in  $E/\Delta$  of changing the wave peak length from 0 to 15 mm, the  $E/\Delta$  increases by 6.5%. Finally for W16, the maximum energy-to-deflection ratio is at wave peak length of 10 mm. In comparing the increase in  $E/\Delta$  of changing the wave peak length from 0 to 10 mm, the  $E/\Delta$  increases by 6.7%. This is attributed to the bond failure between FRP layers that has happened in the analyzed panels. Therefore, increasing the wave peak length increases the bonding area which increases the panels' performance. Having obtained the best results from the above mentioned analyses, a new comparison is conducted. This comparison is between W5 (with  $b = 0$ ) which has the same sinusoidal and flat layers' dimensions as the experimental panels and W16 (with  $b = 10$  mm) which has obtained the best results. As a result in Figure 8, the  $E/\Delta$  increases by 34.3%.

## 6. Conclusions

The effectiveness of new FRP honeycomb sandwich panels in the blast load resistance has been investigated. Throughout this study, a proposed FRP panel with different inner core configurations has been analyzed. The panels' behavior is evaluated using a nonlinear explicit finite element simulation. The numerical model has been validated using experimental field tests conducted on four FRP honeycomb panels filled with sand and subjected to blast effects. The numerical results have shown good agreement with the experimental measurements. The proposed panel has led to a superior performance under blast effects as it increases the energy dissipation by 111% and reduces the level of deformation by 7%.

The parametric studies have been carried out to determine the effect of various parameters: thickness of layers, height of sinusoidal layer, length of sinusoidal wave, width of strip and length of wave peak. While the performance of the simulated panels are evaluated in terms of the panel's peak deflection, energy dissipation and energy-to-deflection ratio ( $E/\Delta$ ). The following results have been observed:

- Changing one of the parameters from H, L, W and T while keeping other parameters constant have resulted in changing the material weight which makes it difficult to compare the results of different panels.
- Having the same material weight, then decreasing the wave length increases the bonds contacts, while decreasing the layers' heights increases the number of layers. Resultantly, the performance of the analyzed panel is enhanced by up to 24.2% increase in the energy dissipation and 1.5% decrease in the panels' peak deflection.
- Changing the wave peak length while keeping the material weight constant, the bonding area increases which improves the performance of the analyzed panel by up to 12.7% in the energy-to-deflection ratio.
- Changing the wave peak length and the other parameters (H, L, W and T) while keeping the material weight constant increase the energy-to-deflection ratio by 34.3%. To conclude, W16 (with  $b = 10$  mm) performs the best among all other panels.

**Table 3.** Effect of changing sinusoidal dimensions with constant weight

Panel	h (mm)	L (mm)	W (mm)	t (mm)	No. of layers	Energy dissipation (J)	$\Delta_{max}$ (mm)	E/ $\Delta$	% E/ $\Delta$
W5	50	100	33	10	4	256	67	3.8	-
W14		80	23	10		261	66	4	+4.0
W15	30	100	33	6.8	6	308	69	4.5	+17.5
W16		80	23	6.8		318	66	4.8	+26.8
W17	110	100	36	15	2	192	81	2.4	-37.6
W18		80	25	13.8		220	79	2.8	-26.7

## 7. References

- Zhou X, Hao H. International Journal of Impact Engineering. 2008 May; 35(5):363–75.
- Hoemann JM. Experimental evaluation of structural composites for blast resistant design. Columbia: University of Missouri; 2007.
- Baker CPA, Westine WE, Kulesz PS, Strehlow JJ. Explosion hazards and valuation. New York, USA: Elsevier Scientific Publishing Company; 1983.
- Vinson JR. Sandwich structures. Applied Mechanics Reviews. 2001 May; 54(3):201–14.
- Davies J. Sandwich panels. Thin-Walled Structures. 1993; 16:179–98.
- Steeves CA, Fleck NA. Material selection in sandwich beam construction. Scripta Materialia. 2004; 50:1335–9.
- Mashadi B, Mahmoodi-k M, Kakaee AH, Hoseini R. Vehicle path following control in the presence of driver inputs. P I Mech Eng K-J Mds. 2013 Jun; 227:115–32.
- Davalos JF, Qiao P, Xu XF, Robinson J, Barth KE. Modeling and characterization of fiber-reinforced plastic honeycomb sandwich panels for highway bridge applications. Composite Structures. 2001 May; 52(3): 441–52.
- Alagusundaramoorthy P, Harik I, Choo C. Structural behavior of FRP composite bridge deck panels. Journal of Bridge Engineering. 2006; 11(4):384–93.
- Ji HS, Song W, Ma ZJ. Design, test and field application of a GFRP corrugated-core sandwich bridge. Engineering Structures. 2010; 32(9):2814–24.
- Sathish U, Lewlyn R, Rodrigues RL. Controlling process factors to optimize surface quality in drilling of GFRP composites by integrating DoE, ANOVA and RSM techniques. Indian Journal of Science and Technology. 2015 Nov; 8(29):23–34.
- Xue Z, Hutchinson JW. A comparative study of impulse-resistant metal sandwich plates. International Journal of Impact Engineering. 2004; 30:1283–305.
- Jacob GC, Fellers JF, Simunovic S, Starbuck JM. Energy absorption in polymer composites for automotive crash worthiness. Journal of Composite Materials. 2002 Apr; 36(7):813–50.
- Zhou G, Hill M, Hookham N. Investigation of parameters governing the damage and energy absorption characteristics of honeycomb sandwich panels. Journal of Sandwich Structures and Materials. 2007 Jul; 9(4):309–42.
- Su H, McConnell J. Influences of material properties on energy absorption of composite sandwich panels under blast loads. Journal of Composites for Construction. 2012 Aug; 16(4):464–74.
- Langdon G, von Klemperer C, Rowland B, Nurick G. The response of sandwich structures with composite face sheets and polymer foam cores to air-blast loading: Preliminary experiments. Engineering Structures. 2012 Mar; 36:104–12.
- Yazici M, Wright J, Bertin D, Shukla A. Experimental and numerical study of foam filled corrugated core steel sandwich structures subjected to blast loading. Composite Structures. 2014 Apr; 110(1):98–109.
- Mahmoodi-k M, Davoodabad D, Visnjic V, Afkar A. Stress and dynamic analysis of optimized trailer chassis. Technical Gazette. 2014 Jun; 21(3):599–608.
- AUTODYNA. Interactive non-linear dynamic analysis software. Version 15, User's Manual. SAS IP Inc. 2014.
- Montazeri-Gh M, Mahmoodi-k M. Development a new power management strategy for power split hybrid electric



- vehicles. *Transportation Research Part D: Transport and Environment*. 2015 May; 37:79–96.
21. Rajamurugan TV, Shanmugam K, Palanikumar K. Mathematical model for predicting thrust force in drilling of GFRP composites by multifaceted drill. *Indian Journal of Science and Technology*. 2013 Oct; 6(10):1–9.
  22. Kalny O, Peterman RJ. Performance investigation of a fiber reinforced composite honeycomb deck for bridge applications. 2005 Jun.